arXiv:1512.03447v1 [cond-mat.quant-gas] 10 Dec 2015

Anderson localization of Cooper pairs and Majorana fermions in an ultracold atomic Fermi gas with synthetic spin-orbit coupling

Ye Cao[1], Gao Xianlong[2], Xia-Ji Liu[1], and Hui Hu[1]
[1] *Centre for Quantum and Optical Science, Swinburne University of Technology, Melbourne 3122, Australia and*
[2] *Department of Physics, Zhejiang Normal University, Jinhua 321004, China*

(Dated: December 14, 2015)

We theoretically investigate two-particle and many-particle Anderson localizations of a spin-orbit coupled ultracold atomic Fermi gas trapped in a quasi-periodic potential and subjected to an out-of-plane Zeeman field. We solve exactly the two-particle problem in a finite length system by exact diagonalization and solve approximately the many-particle problem within the mean-field Bogoliubov-de Gennes approach. At a small Zeeman field, the localization properties of the system are similar to that of a Fermi gas with conventional s-wave interactions. As the disorder strength increases, the two-particle binding energy increases and the fermionic superfluidity of many particles disappears above a threshold. At a large Zeeman field, where the interatomic interaction behaves effectively like a p-wave interaction, the binding energy decreases with increasing disorder strength and the resulting topological superfluidity shows a much more robust stability against disorder than the conventional s-wave superfluidity. We also analyze the localization properties of the emergent Majorana fermions in the topological phase. Our results could be experimentally examined in future cold-atom experiments, where the spin-orbit coupling can be induced artificially by using two Raman lasers, and the quasi-periodic potential can be created by using bichromatic optical lattices.

PACS numbers: 05.30.Fk, 03.75.Hh, 03.75.Ss, 67.85.-d

Ultracold atomic Fermi gases provide one of the most versatile platforms for realizing exotic many-body quantum states of matter, due to their unprecedented tunability and controllability [1, 2]. Strongly interacting Fermi gases are easily achievable through the use of Feshbach resonances [3], which enable the realization of the crossover from Bose-Einstein condensates (BEC) to Bardeen-Cooper-Schrieffer (BCS) superfluids [2]. Low-dimensional Fermi gases are accessible by imposing optical lattice potentials [4–6], potentially allowing the observation of the elusive antiferromagnetic Néel order in the fermionic Hubbard model [7]. Two more examples are the recently synthesized spin-orbit coupled Fermi gases [8–10] and quasi-disordered Fermi gases in bichromatic optical lattices [11, 12], which open the ways to realize topological superfluids [13–16] and many-body localizations [11, 12, 17], respectively.

In this Rapid Communication, motivated by these rapid experimental progress, we propose to investigate Anderson localization of two and many interacting fermions in one-dimensional (1D) quasi-disordered lattices, in the presence of a synthetic spin-orbit coupling and an out-of-plane Zeeman field. By increasing the strength of the Zeeman field above a threshold, the underlying character of the effective interatomic interaction changes from s-wave to p-wave [18], and in the absence of disorder the many-fermion system is known to experience a topological phase transition [13–15]. The main purpose of this work is to determine a rich phase diagram due to the interplay between disorder and s-wave or p-wave superfluidity.

Under sufficiently strong disorder potential, a dirty s-wave superconductors such as a superconducting NbN thin film undergoes a quantum phase transition towards a gapped insulator [19]. In condensed matter physics, such a superconductor-insulator transition has attracted a lot of interests over the past two decades [20–25]. Yet, a complete understanding of the transition remains elusive. Also, the behavior of a dirty p-wave superconductor and its phase transition towards a gapped insulator is less known [26–28]. Our proposed system of disordered spin-orbit coupled atomic Fermi gases offers an unique opportunity to better understand these quantum phase transitions. In particular, it is of great interest to determine how does disorder affect the topological phase transition and how is the fate of Majorana fermion edge modes - as the key feature of a topological superfluid - against disorder. Naïvely, we may anticipate two differ-

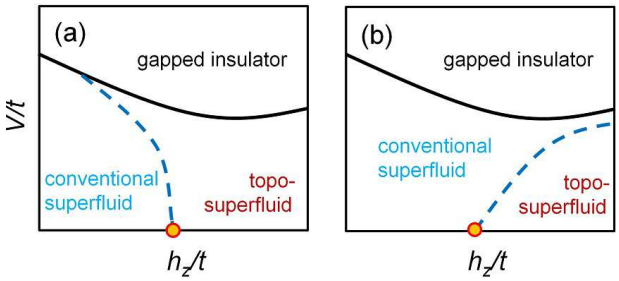

FIG. 1: (color online) Two possible phase diagrams for a spin-orbit coupled Fermi gas in a disordered potential. In the first-type diagram (a), as the disorder strength increases, a conventional s-wave superfluid turns into a topological superfluid before losing its superfluidity. The transition from a topological superfluid to a gapped insulator is direct. In contrast, in the second-type diagram (b), with increasing disorder strength a topological superfluid first becomes a conventional superfluid and then translates into a gapped insulator.

ent phase diagrams, as schematically illustrated in Fig. 1. As the disorder strength increases, the topological phase transition line (the dashed curve) could bend to either the left or right hand side of the circle that indicates the initial transition point in the clean limit. In other words, with increasing disorder, an s-wave superfluid may first become a topological superfluid before it finally turns into a gapped insulator (i.e., the scenario a), or vice versa (b).

The proposed 1D spin-orbit coupled Fermi system in quasi-disordered lattices can be easily realized in cold-atom laboratory, where the synthetic spin-orbit coupling and disorder potential can be created by using Raman laser beams and bichromatic optical lattices [29], respectively. By using the self-consistent Bogoliubov-de Gennes mean-field theory, we calculate the superfluid density (under periodic boundary condition) and the Majorana fermion edge modes (with open boundary condition) of the system at zero temperature. A vanishingly small superfluid density indicates the transition to a gapped insulator, while the existence of Majorana fermions signals the topological phase transition. This allows us to determine the whole phase diagram (see Fig. 4), the main result of this work. To understand the phase diagram, we exactly solve the two-fermion problem and address the Anderson localization of a Cooper pair in its ground state [30]. To utilize and better understand the robustness of Majorana fermions with respect to disorder, we also consider the soliton-induced Majorana fermions [31, 32] and investigate the evolution of their energies and wavefunctions as a function of the disorder strength. Our results on the Anderson localization of Majorana fermions may be useful for manipulating these exotic non-abelian quasi-particles in realistic noisy environment, for the purpose of performing fault-tolerant quantum information processing [33].

Model Hamiltonian. — We start by considering a 1D disordered spin-orbit coupled Fermi gas in a lattice with L sites. The system can be described by the fermionic model Hamiltonian,

$$\begin{aligned}\mathcal{H} &= -t\sum_{i=1}^{L}\sum_{\sigma}\left(\boldsymbol{c}_{i+1,\sigma}^{\dagger}\boldsymbol{c}_{i,\sigma}+\text{H.c.}\right)+\sum_{i,\sigma}V_i\boldsymbol{n}_{i\sigma}\\ &\quad+\mathcal{H}_R+\mathcal{H}_Z-U\sum_{i}\boldsymbol{n}_{i\uparrow}\boldsymbol{n}_{i\downarrow},\end{aligned}\tag{1}$$

where $\boldsymbol{c}_{i\sigma}$ is the annihilation operator with spin $\sigma\in\{\uparrow,\downarrow\}$ at site i, $\boldsymbol{n}_{i\sigma}=\boldsymbol{c}_{i\sigma}^{\dagger}\boldsymbol{c}_{i\sigma}$ is the local number operator, t is the tunneling strength between neighboring lattice sites, $V_i=V\cos(2\pi\beta i+\phi)$ with an irrational number β and phase offset ϕ describes the quasi-random disorder potential induced by bichromatic (i.e., additional incommensurate) lattices [11, 12], and $U>0$ in the last term represents the on-site attractive interaction. For definiteness, we shall take $\beta=(\sqrt{5}-1)/2$ and $\phi=0$. We assume a periodic boundary condition such that $\boldsymbol{c}_{L+1,\sigma}=\boldsymbol{c}_{1\sigma}$, unless specified otherwise. Finally, the spin-orbit term with Rashba-type coupling $\mathcal{H}_R$ and the Zeeman energy term $\mathcal{H}_Z$ are given by,

$$\mathcal{H}_R = \frac{\lambda}{2}\sum_{i=1}^{L}\left(\boldsymbol{c}_{i+1,\downarrow}^{\dagger}\boldsymbol{c}_{i\uparrow}-\boldsymbol{c}_{i+1,\uparrow}^{\dagger}\boldsymbol{c}_{i\downarrow}+\text{H.c.}\right),\tag{2}$$

$$\mathcal{H}_Z = h_z\sum_{i=1}^{L}\left(\boldsymbol{c}_{i\uparrow}^{\dagger}\boldsymbol{c}_{i\uparrow}-\boldsymbol{c}_{i\downarrow}^{\dagger}\boldsymbol{c}_{i\downarrow}\right),\tag{3}$$

respectively. Here, λ is the spin-orbit coupling strength and h_z is the Zeeman field.

We note that, in the absence of $\mathcal{H}_R$ and $\mathcal{H}_Z$, the model Hamiltonian Eq. (1) - known as Aubry-André-Harper model [34, 35] - has been experimentally explored [11]. In the non-interacting limit ($U=0$), all single-particle states become localized at the same critical disorder strength $V=2t$ [35]. For an initial charge density-wave state, its many-body localization at arbitrary U has been demonstrated [11]. The possibility of having the spin-orbit and Zeeman terms in the model Hamiltonian was recently proposed and derived by Zhou and co-workers [29]. The Anderson localization of a single atom in the non-interacting limit (U=0) was studied. It was found that the spin-orbit coupling can lead to a non-pure spectrum (i.e., coexistence of extended and localized states) and the appearance of mobility edges. Here, we are interested in the localization of the many-body ground state and the interplay between disorder and conventional/unconventional superfluidity.

Localization of a single Cooper pair. — Before discussing the localization of the coherent (superfluid) state of many Cooper pairs, it is instructive to understand the localization of a single Cooper pair [30]. For this purpose, we numerically exactly solve the two-fermion problem:

$$(\mathcal{H}-E)\sum_{i,j}\left[\psi_{ij}^{\uparrow\uparrow}\boldsymbol{c}_{i\uparrow}^{\dagger}\boldsymbol{c}_{j\uparrow}^{\dagger}+\psi_{ij}^{\uparrow\downarrow}\boldsymbol{c}_{i\uparrow}^{\dagger}\boldsymbol{c}_{j\downarrow}^{\dagger}+\psi_{ij}^{\downarrow\downarrow}\boldsymbol{c}_{i\downarrow}^{\dagger}\boldsymbol{c}_{j\downarrow}^{\dagger}\right]|0\rangle=0,\tag{4}$$

where $\psi_{ij}^{\sigma\sigma'}$ is the two-particle wave-function and E is the energy. It is understood that for the same spin $\sigma=\sigma'$ at the same site $i=j$, $\psi_{ij}^{\sigma\sigma'}=0$ because of Pauli exclusion principle. For numerical stability, we approximate the irrational number β as the limit of a continued fraction, $\beta\simeq F_{l-1}/F_l$, where F_l are Fibonacci numbers and l is a sufficiently large integer. We minimize the finite-size effect by taking the length of the lattice $L=F_l$ [30]. To characterize the Anderson localization of the pair, we use the inverse participation ratio (IPR) [36],

$$\alpha_{\text{IPR}}=\sum_{i,j}\left(\left|\psi_{ij}^{\uparrow\uparrow}\right|^4+\left|\psi_{ij}^{\uparrow\downarrow}\right|^4+\left|\psi_{ij}^{\downarrow\downarrow}\right|^4\right).\tag{5}$$

For an extended state, $\alpha_{\text{IPR}}\propto 1/L^2$ decreases to zero in the thermodynamic limit. While for a localized state, it saturates to a finite value.

We have calculated α_{IPR} for the ground state of the pair at a moderate interaction $U=4.5t$ and spin-orbit coupling $\lambda=2t$, as reported in the phase diagram Fig.

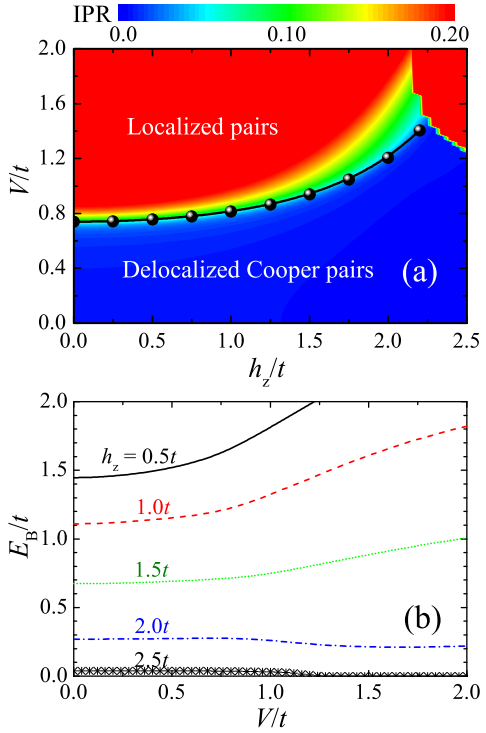

FIG. 2: (color online) (a) Anderson localization of Cooper pairs, indicated by the inverse participation ratio (IPR) of the ground state two-particle wave-function at $L = F_{l=10} = 89$. The black circles with line shows the phase boundary in the rational limit $L \to \infty$. (b) Binding energy of the ground state Cooper pair as a function of the disorder strength at several Zeeman fields. Here, we set $U = 4.5t$ and $\lambda = 2t$.

2a. As the disorder strength V increase, there is a sharp increase in the IPR. We then identify the critical strength $V_{c,2p}$ as the inflection point of the calculated curve $\alpha_{\rm IPR}(V)$. By repeating calculations at different lengths of lattices (up to $L = F_{12} = 233$), we eliminate the finite-size dependence and determine the phase boundary $V_{c,2p}$ in the thermodynamic limit, as shown by solid circles in the figure. It is interesting that with increasing Zeeman field, the threshold $V_{c,2p}$ increases. This might be understood from the fact that a finite Zeeman field plays a role of pair breaker and the resulting weakly bound pair is easier to move in disordered potential than a tightly bound pair [30]. In Fig. 2b, we present the binding energy $E_B = 2\epsilon_1 - E$ of the pair as a function of the disorder strength at different Zeeman fields. Here ϵ_1 is the ground state energy for a single fermion. Indeed, with increasing Zeeman field, the binding energy decreases quickly. As a result, at sufficiently large Zeeman field, a Cooper pair may break into two fermions. This pair breaking effect is mostly evident at $h_z = 2.5t$, where the pair creases to exist at $V \gtrsim 1.2t$. In this part of parameter space (i.e., the top-right part of Fig. 2a), actually we observe the Anderson localization of a single fermion instead of a Cooper pair [29].

It is also worth noting that the binding energy shows very different dependence on the disorder strength at small and large Zeeman fields. While the disorder enhances the binding energy at low Zeeman field, it breaks pair at high field. These two distinct behaviors may be attributed to the different effective interatomic interactions. For a spin-orbit coupled Fermi gas, with increasing Zeeman field, the underlying interaction between atoms changes from s-wave like to p-wave like with increasing the Zeeman field above a threshold [18]. For the parameter used in Fig. 2b, this transition occurs at about $h_z \sim 1.8t$.

Mean-field phase diagram. — We now turn to consider the ground state of many fermions by using mean-field Bogoliubov-de Gennes theory, which is known to capture the qualitative physics in low dimensions [21]. To this aim, we decouple the interaction term $-U\sum_i \boldsymbol{n}_{i\uparrow}\boldsymbol{n}_{i\downarrow}$ into the pairing term and the Hartree-Fock term, $\mathcal{H}_\Delta = \sum_i(\Delta_i \boldsymbol{c}^\dagger_{i\uparrow}\boldsymbol{c}^\dagger_{i\downarrow} + \Delta^*_i \boldsymbol{c}_{i\downarrow}\boldsymbol{c}_{i\uparrow} + |\Delta_i|^2/U)$ and $\mathcal{H}_{\rm HF} = \sum_i(-U\langle\boldsymbol{n}_{i\uparrow}\rangle\boldsymbol{n}_{i\downarrow} - U\langle\boldsymbol{n}_{i\downarrow}\rangle\boldsymbol{n}_{i\uparrow} + U\langle\boldsymbol{n}_{i\uparrow}\rangle\langle\boldsymbol{n}_{i\downarrow}\rangle)$, which yields an effective quadratic Hamiltonian,

$$\begin{aligned}\mathcal{H}_{\rm eff} &= -t\sum_{i\sigma}\left(\boldsymbol{c}^\dagger_{i+1,\sigma}\boldsymbol{c}_{i,\sigma} + \text{H.c.}\right) + \sum_{i,\sigma}(V_i - \tilde{\mu}_{i\bar{\sigma}})\,\boldsymbol{n}_{i\sigma} \\ &\quad + \mathcal{H}_R + \mathcal{H}_Z + \sum_i\left(\Delta_i \boldsymbol{c}^\dagger_{i\uparrow}\boldsymbol{c}^\dagger_{i\downarrow} + \text{H.c.}\right) + E_0, \quad (6)\end{aligned}$$

where $E_0 = \sum_i(|\Delta_i|^2/U + U\langle\boldsymbol{n}_{i\uparrow}\rangle\langle\boldsymbol{n}_{i\downarrow}\rangle)$ is a constant and $\tilde{\mu}_{i\sigma} = \mu + U\langle\boldsymbol{n}_{i\sigma}\rangle$ is the local chemical potential that incorporates the site-dependent Hartree shift. We diagonalize the effective Hamiltonian by using the standard Bogoliubov transformation, which leads to,

$$\begin{bmatrix} \hat{K}_+ & \hat{\Lambda}^\dagger & 0 & \hat{\Delta} \\ \Lambda & \hat{K}_- & -\hat{\Delta} & 0 \\ 0 & -\hat{\Delta}^* & -\hat{K}^*_+ & -\hat{\Lambda}^{\dagger *} \\ \hat{\Delta}^* & 0 & -\Lambda^* & -\hat{K}^*_- \end{bmatrix} \begin{bmatrix} u^{(\eta)}_{i\uparrow} \\ u^{(\eta)}_{i\downarrow} \\ v^{(\eta)}_{i\uparrow} \\ v^{(\eta)}_{i\downarrow} \end{bmatrix} = E_\eta \begin{bmatrix} u^{(\eta)}_{i\uparrow} \\ u^{(\eta)}_{i\downarrow} \\ v^{(\eta)}_{i\uparrow} \\ v^{(\eta)}_{i\downarrow} \end{bmatrix}, \quad (7)$$

where $u^{(\eta)}_{i\sigma}$ and $v^{(\eta)}_{i\sigma}$ are the Bogoliubov quasiparticle wavefunctions and E_η is the associated quasiparticle energy. The operators $\hat{K}_\pm = \hat{K} \pm h_z$, Λ, and $\hat{\Delta}$ are respectively given by,

$$\begin{aligned}\hat{K}u^{(\eta)}_{i\sigma} &= -t\left[e^{-i\theta}u^{(\eta)}_{i+1,\sigma} + e^{i\theta}u^{(\eta)}_{i-1,\sigma}\right] + (V_i - \tilde{\mu}_{i\bar{\sigma}})\,u^{(\eta)}_{i\sigma}, \\ \hat{\Lambda}u^{(\eta)}_{i\uparrow} &= +(\lambda/2)\left[e^{-i\theta}u^{(\eta)}_{i+1,\downarrow} - e^{i\theta}u^{(\eta)}_{i-1,\downarrow}\right], \\ \hat{\Lambda}^\dagger u^{(\eta)}_{i\downarrow} &= -(\lambda/2)\left[e^{-i\theta}u^{(\eta)}_{i+1,\uparrow} - e^{i\theta}u^{(\eta)}_{i-1,\uparrow}\right], \\ \hat{\Delta}u^{(\eta)}_{i\sigma} &= \Delta_i u^{(\eta)}_{i\sigma}, \end{aligned} \quad (8)$$

and similarly for $v^{(\eta)}_{i\sigma}$. The local pairing gap and local density are determined by the self-consistency conditions,

$$\begin{aligned}\Delta_i &= -U\sum_\eta\left[u^{(\eta)}_{i\uparrow}v^{(\eta)*}_{i\downarrow}f(E_\eta) + u^{(\eta)}_{i\downarrow}v^{(\eta)*}_{i\uparrow}f(-E_\eta)\right], \\ \langle\boldsymbol{n}_{i\sigma}\rangle &= \sum_\eta\sum_\sigma\left[\left|u^{(\eta)}_{i\sigma}\right|^2 f(E_\eta) + \left|u^{(\eta)}_{i\sigma}\right|^2 f(-E_\eta)\right], \end{aligned} \quad (9)$$

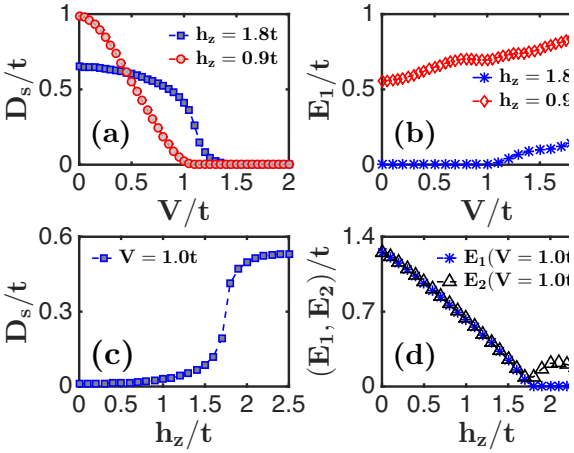

FIG. 3: (color online) Left panel: Evolution of the superfluid stiffness as a function of the disorder strength (a) or Zeeman field strength (c). Right panel: The lowest or the second lowest quasiparticle excitation energy as a function of the disorder strength (b) or Zeeman field strength (d), under an open boundary condition. Here, we take $L = 89$ and set $U = 4.5t$ and $\lambda = 2t$. Moreover, we use an average (quarter) filling factor $n = N/L = 44/89$.

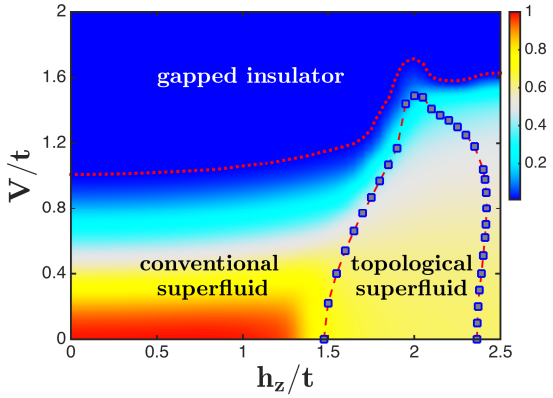

FIG. 4: (color online) Phase diagram of a 1D spin-orbit coupled Fermi gas in bichromatic optical lattices at $U = 4.5t$ and $\lambda = 2t$. The color bar indicates the superfluid stiffness. A vanishingly small superfluid stiffness (i.e., the red dotted line) determines the phase transition to a normal state (V_c), due to the many-body Anderson localization of the ground state. The blue squares with dashed line (V_c^*) enclose the phase space, where the superfluid is topologically non-trivial and Majorana fermions exist at the two open edges. The other parameters are the same as in Fig. 3.

where $f(E_\eta) = 1/(e^{E_\eta/k_BT} + 1)$ is the Fermi-Dirac distribution function. Throughout the paper, we focus on the zero-temperature case where $f(E_\eta)$ becomes a step function.

We note that in defining the operators $\hat{K}$ and $\hat{\Lambda}$, a phase twist θ is explicitly added, which corresponds to introduce a constant vector potential $\theta_i = \theta$ across the system [37]. This implementation is convenient for the calculation of the superfluid stiffness D_s. Indeed, with the vector potential, D_s is given by the change in the free energy $F = \langle \mathcal{H}_{\rm eff} \rangle + \mu N$ [25]:

$$D_s = \frac{1}{L} \frac{\partial^2 F(\theta)}{\partial \theta^2}. \tag{10}$$

It is necessary to use such a formal expression in the presence of disorder, since the decoupling between longitudinal and transverse electromagnetic responses does not hold and the standard approach of calculating D_s through the BCS response function fails [25].

For the localization of many fermions in their ground state, we use a vanishingly small superfluid stiffness to characterize a gapped insulator phase. Alternatively, we may also determine the onset of the localization phase through the calculation of the IPR of Bogoliubov quasiparticle wavefunctions, as in the case of two fermions. However, the use of exponentially small superfluid stiffness turns out to be a more physical criterion. On the other hand, as we mentioned earlier, the system features a topological superfluid at relatively large Zeeman fields. While the existence of a non-trivial topology of the superfluid can be revealed by some topological invariants [15], numerically it is actually more convenient to be identified from the appearance of two Majorana fermion modes at the edges, if one imposes an open boundary condition.

In the left panel of Fig. 3, we report the superfluid stiffness as a function of the disorder strength and of the Zeeman field. The corresponding results for the energy of low-lying quasiparticle modes are shown in the right panel of the figure. At a given Zeeman field (Fig. 3a), the superfluid stiffness vanishes exponentially above a critical value V_c, signifying the transition towards a gapped insulator. The energy of low-lying modes exhibits different dependence on disorder strength at low and high Zeeman fields (Fig. 3b). At a small Zeeman field $h_z = 0.9t$, the energy gap ($E_{\rm gap} = 2E_1$) is always nonzero and increases monotonically with disorder strength, as anticipated for a disordered conventional s-wave superfluid [21]. In contrast, at a large Zeeman field $h_z = 1.8t$, there are two zero-energy modes that correspond to the Majorana fermions localized at the two edges. By increasing the disorder strength above a threshold V_c^*, the zero-energy modes crease to exist [27, 28], suggesting the loss of the non-trivial topological property of the superfluid. The two critical disorder strengths, V_c and V_c^*, do not necessarily take the same value.

By collecting the two critical disorder strengths at different Zeeman fields, we arrive at our main result - the phase diagram of a spin-orbit coupled Fermi gas in quasi-random lattices - as illustrated in Fig. 4. It is remarkable that the many-body localization strength V_c (i.e., the red dotted line) follows very closely behind the two-particle localization strength $V_{c,2p}$. This indicates that the loss of coherence between Cooper pairs and the localization of pairs occurs nearly at the same time. It is also interesting that, in the presence of disorder, we find a large parameter space to accommodate topological superflu-

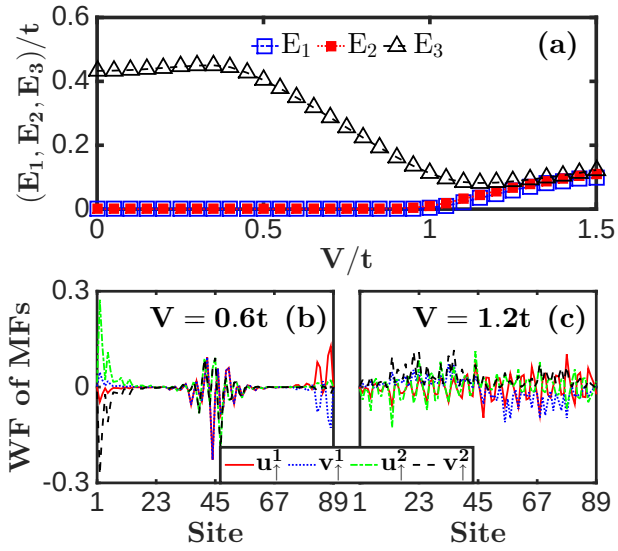

FIG. 5: (color online) Upper panel: Evolution of the three lowest quasiparticle excitation energies as a function of the disorder strength, under an open boundary condition and in the presence of a soliton at the center of the system. Lower panel: The wave functions of the two Majorana fermions (E_1 and E_2) at the disorder strength $V = 0.6t$ (b) and $V = 1.2t$ (c). Here, we fix the Zeeman field strength to $h_z = 1.8t$. The other parameters are the same as in Fig. 3.

ids. In particular, a topological superfluid appears to be more robust against disorder than a conventional s-wave superfluid. There is no direct transition from a topological superfluid to the gapped insulator. Therefore, the scenario (b) in the schematical phase diagram Fig. 1 is favored.

Anderson localization of Majorana fermions. —We now examine in more detail the localization of Majorana fermions, which gives the critical strength V_c^*. Experimentally, it seems convenient to create and manipulate Majorana fermions by engineering solitons via the phase-imprinting technique [38, 39]. At the site of each soliton, there exist two soliton-induced Majorana fermions [31, 32]. In Fig. 5, we plot the energy and wavefunctions of low-lying quasiparticle modes in the presence of a dark soliton at the center of the topological superfluid and under an open boundary condition [40]. The wave-functions of Majorana fermions are essentially not affected by a weak or moderately strong disorder (Fig. 5b) and are well localized at the edges or at the site of soliton. Towards the critical strength V_c^* (Fig. 5c), however, the wave-functions spread over the whole lattice sites. Majorana fermions disappear, although the quasiparticle states are still extensive.

Conclusions. —We have proposed to study the Anderson localization of a spin-orbit coupled Fermi gas in one-dimensional quasi-disordered lattices. In the absence of disorder, the system features a conventional s-wave-like superfluid and topological p-wave-like superfluid at small and large Zeeman fields [18], respectively. By tuning the Zeeman field, we have investigated how these superfluid states lose their superfluidity with increasing disorder strength. We have found that topological superfluids (and hence the hosted Majorana fermions) are very robust against disorder and they lose their non-trivial topological properties before finally turn into gapped insulators. We have complemented our many-body study by considering the localization of a single Copper pair. The result indicates that the localization of pairs and the loss of coherence between pairs occurs simultaneously.

In the near future, it is of interest to consider Anderson localization of the spin-orbit coupled Fermi gas system in two-dimensional disordered lattices [12]. The strong quantum phase fluctuations near topological and localization transitions could be addressed by using a zero-temperature Gaussian fluctuation theory [41–43].

Acknowledgments

GX was supported by the NSF of China (Grant Nos. 11374266 and 11174253) and the Program for New Century Excellent Talents in University. XJL and HH were supported by the ARC Discovery Projects (Grant Nos. FT130100815, DP140103231, FT140100003, and DP140100637) and NFRP-China (Grant No. 2011CB921502).

[1] I. Bloch, J. Dalibard, W. Zwerger, Rev. Mod. Phys. **80**, 885 (2008).
[2] S. Giorgini, L. P. Pitaevskii, and S. Stringari, Rev. Mod. Phys. **80**, 1215 (2008).
[3] C. Chin, R. Grimm, P. Julienne, and E. Tiesinga, Rev. Mod. Phys. **82**, 1225 (2010).
[4] Y. A. Liao, A. S. C. Rittner, T. Paprotta, W. Li, G. B. Partridge, R. G. Hulet, S. K. Baur, and E. J. Mueller, Nature **467**, 567 (2010).
[5] K. Martiyanov, V. Makhalov, and A. Turlapov, Phys. Rev. Lett. **105**, 030404 (2010).
[6] G. Pagano, M. Mancini, G. Cappellini, P. Lombardi, F. Schäfer, H. Hu, X.-J. Liu, J. Catani, C. Sias, M. Inguscio, and L. Fallani, Nature Phys. **10**, 198 (2014).
[7] R. A. Hart, P. M. Duarte, T.-L. Yang, X. Liu, T. Paiva, E. Khatami, R. T. Scalettar, N. Trivedi, D. A. Huse, and R. G. Hulet, Nature (London) **519**, 211 (2015).
[8] P. Wang, Z. Yu, Z. Fu, J. Miao, L. Huang, S. Chai, H. Zhai, and J. Zhang, Phys. Rev. Lett. **109**, 095301 (2012).
[9] L. W. Cheuk, A. T. Sommer, Z. Hadzibabic, T. Yefsah, W. S. Bakr, and M. W. Zwierlein, Phys. Rev. Lett. **109**, 095302 (2012).
[10] Z. Fu, L. Huang, Z. Meng, P. Wang, X.-J. Liu, H. Pu, H. Hu, and J. Zhang, Phys. Rev. A **87**, 053619 (2013).
[11] M. Schreiber, S. S. Hodgman, P. Bordia, H. P. Lüschen, M. H. Fischer, R. Vosk, E. Altman, U. Schneider, and I.

Bloch, Science **349**, 842 (2015).
[12] P. Bordia, H. P. Lüschen, S. S. Hodgman, M. Schreiber, I. Bloch, and U. Schneider, arXiv:1509.00478 (2015).
[13] X.-J. Liu, L. Jiang, H. Pu, and H. Hu, Phys. Rev. A **85**, 021603(R) (2012).
[14] X.-J. Liu and H. Hu, Phys. Rev. A **85**, 033622 (2012).
[15] R. Wei and E. J. Mueller, Phys. Rev. A **86**, 063604 (2012).
[16] For a recent review, see, for example, J. Zhang, H. Hu, X.-J. Liu, and H. Pu, Annu. Rev. Cold At. Mol. **2**, 81 (2014).
[17] D. M. Basko, I. L. Aleiner, B. L. Altshuler, Ann. Phys. **321**, 1126 (2006).
[18] C. Zhang, S. Tewari, R. M. Lutchyn, and S. Das Sarma, Phys. Rev. Lett. **101**, 160401 (2008).
[19] M. Mondal, A. Kamlapure, M. Chand, G. Saraswat, S. Kumar, J. Jesudasan, L. Benfatto, V. Tripathi, and P. Raychaudhuri, Phys. Rev. Lett. **106**, 047001 (2011).
[20] M. Ma and P. A. Lee, Phys. Rev. B **32**, 5658 (1985).
[21] A. Ghosal, M. Randeria, and N. Trivedi, Phys. Rev. B **65**, 014501 (2001).
[22] M. V. Feigelman, L. B. Ioffe, V. E. Kravtsov, and E. A. Yuzbashyan, Phys. Rev. Lett. **98**, 027001 (2007).
[23] Y. Dubi, Y. Meir, and Y. Avishai, Nature (London) **449**, 876 (2007).
[24] K. Bouadim, Y. L. Loh, M. Randeria, and N. Trivedi, Nature Phys. **7**, 884 (2011).
[25] G. Seibold, L. Benfatto, C. Castellani, and J. Lorenzana Phys. Rev. Lett. **108**, 207004 (2012).
[26] W. DeGottardi, D. Sen, and S. Vishveshwara, Phys. Rev. Lett. **110**, 146404 (2013).
[27] X. Cai, L.-J. Lang, S. Chen, and Y. Wang, Phys. Rev. Lett. **110**, 176403 (2013).
[28] J. Wang, X.-J. Liu, X. Gao, and H. Hu, arXiv:1505.03646 (2015).
[29] L. Zhou, H. Pu, and W. Zhang, Phys. Rev. A **87**, 023625 (2013).
[30] G. Dufour and G. Orso, Phys. Rev. Lett. **109**, 155306 (2012).
[31] Y. Xu, L. Mao, B. Wu, and C. Zhang, Phys. Rev. Lett. **113**, 130404 (2014).
[32] X.-J. Liu, Phys. Rev. A **91**, 023610 (2015).
[33] C. Nayak, S. Simon, A. Stern, M. Freedman, and S. Das Sarma, Rev. Mod. Phys. **80**, 1083 (2008).
[34] P. G. Harper, Proc. Phys. Soc. London Sect. A **68**, 874 (1955).
[35] S. Aubry and G. André, Ann. Isr. Phys. Soc. **3**, 133 (1980).
[36] F. Evers and A. D. Mirlin, Rev. Mod. Phys. **80**, 1355 (2008).
[37] Using the Peierls substitution, the presence of a constant vector potential θ corresponds to a change in the hopping (kinetic) term $-t\sum_{i\sigma}(e^{-i\theta}\boldsymbol{c}^{\dagger}_{i+1,\sigma}\boldsymbol{c}_{i\sigma}$ + H.c.) and in the spin-orbit coupling term, $\mathcal{H}_R(\theta) = (\lambda/2)\sum_i(e^{-i\theta}\boldsymbol{c}^{\dagger}_{i+1,\downarrow}\boldsymbol{c}_{i\uparrow} - e^{-i\theta}\boldsymbol{c}^{\dagger}_{i+1,\uparrow}\boldsymbol{c}_{i\downarrow} + \text{H.c.})$.
[38] T. Yefsah, A. T. Sommer, M. J. H. Ku, L. W. Cheuk, W. Ji, W. S. Bakr, and M. W. Zwierlein, Nature (London) **499**, 426 (2013).
[39] M. J. H. Ku, B. Mukherjee, T. Yefsah, and M. W. Zwierlein, arXiv:1507.01047 (2015).
[40] Theoretically, a dark soliton at a site A can be created by imposing the following constraint to the local pairing gap: $\Delta_{i<A} > 0$, $\Delta_{i=A} = 0$, and $\Delta_{i>A} < 0$.
[41] H. Hu, X.-J. Liu, and P. D. Drummond, Europhys. Lett. **74**, 574 (2006).
[42] R. B. Diener, R. Sensarma, and M. Randeria, Phys. Rev. A **77**, 023626 (2008).
[43] L. He, H. Lü, G. Gao, H. Hu, and X.-J. Liu, Phys. Rev. A **92**, 023620 (2015).